ACS Medicinal Chemistry Letters

Letter

pubs.acs.org/acsmedchemlett

Minibody-Indocyanine Green Based Activatable Optical Imaging Probes: The Role of Short Polyethylene Glycol Linkers

Rira Watanabe,[†] Kazuhide Sato,[†] Hirofumi Hanaoka,[†] Toshiko Harada,[†] Takahito Nakajima,[†] Insook Kim,[‡] Chang H. Paik,[§] Anna M. Wu,[∥] Peter L. Choyke,[†] and Hisataka Kobayashi*,[†]

[†]Molecular Imaging Program, Center for Cancer Research, National Cancer Institute, National Institutes of Health, Bethesda, Maryland 20892, United States

[‡]Applied/Developmental Research Directorate, Leidos Biomedical Research, Inc., Frederick National Laboratory, Frederick, Maryland 21702, United States

[§]Nuclear Medicine Department, Radiology and Imaging Science, Warren Grant Magnuson Clinical Center, National Institutes of Health, Bethesda, Maryland 20892, United States

[∥]Department of Molecular and Medical Pharmacology, David Geffen School of Medicine at UCLA, Los Angeles, California 90095, United States

Supporting Information

ABSTRACT: Minibodies show rapider blood clearance than IgGs due to smaller size that improves target-to-background ratio (TBR) in in vivo imaging. Additionally, the ability to activate an optical probe after binding to the target greatly improves the TBR. An optical imaging probe based on a minibody against prostate-specific membrane antigen (PSMA-MB) and conjugated with an activatable fluorophore, indocyanine green (ICG), was designed to fluoresce only after binding to cell-surface PSMA. To further reduce background signal, short polyethylene glycol (PEG) linkers were employed to improve the covalent bonding ratio of ICG. New PSMA-MBs conjugated with bifunctional ICG derivatives specifically visualized PSMA-positive tumor xenografts in mice bearing both PSMA-positive and -negative tumors within 6 h postinjection. The addition of short PEG linkers significantly improved TBRs; however, it did not significantly alter the biodistribution. Thus, minibody-ICG conjugates could be a good alternative to IgG-ICG in the optical cancer imaging for further clinical applications.

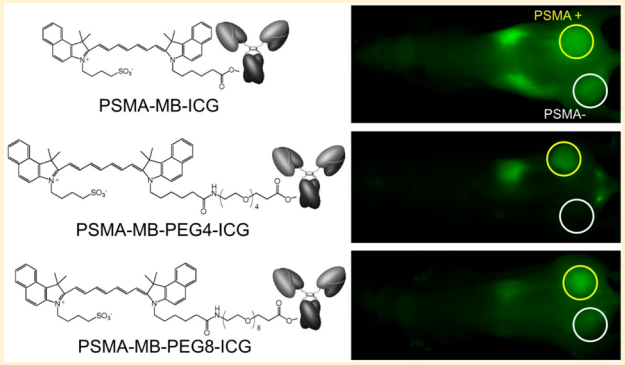

KEYWORDS: *Molecular imaging, minibody, indocyanine green, prostate cancer, near-infrared fluorescence*

Optical imaging probes targeting cancer are becoming increasingly important for guiding endoscopic and surgical procedures,[1,2] and recently, the first in human clinical trials with optical probes were completed.[3] A variety of targeting moieties has been proposed, and these have been conjugated to optical fluorophores to create new optical probes. Among these, monoclonal antibodies (mAbs) show the greatest binding specificity to target antigens, and many therapeutic antibodies are now approved for clinical use.[4] Optically labeled full mAbs have shown some success in in vivo imaging, but they are limited by their long clearance times requiring long delays after injection before imaging can begin.

Because mAb-optical conjugates have long clearance times resulting in high background signal from normal organs, several strategies have been emerged to decrease background signal and thus increase the target to background ratio (TBR). One strategy is to physically reduce the size of the mAb so as to improve its pharmacokinetics. This can be achieved by enzymatically or genetically modifying mAbs to produce Fab and $F(ab)'_2$ fragments, diabodies, and minibodies.[5] Since the clearance time of these smaller antibody fragments is shorter, they can be used as targeting moieties to minimize background signals.[6−8]

Another strategy to achieve higher TBR is to make the optical probe activatable so that it is turned off in the absence of binding and is turned on only after binding to the cognate antigen on the target cell and internalization.[9,10] A large number of potentially activatable dyes exist; however, few have actually been tested in humans. Indocyanine green (ICG) is a quenchable near-infrared (NIR) fluorophore that has been in clinical use for many decades as a contrast agent for retinal angiography and liver function studies. When a full mAb is conjugated to a bifunctional ICG derivative, in which one sulfonic acid is replaced with a carboxylic acid so as to permit

Received: December 27, 2013
Accepted: January 17, 2014
Published: January 17, 2014

conjugation with an amino group of the mAb, the ICG molecules are highly quenched.[11] ICG autoquenches as a result of interactions between the ICG and aromatic amino acids on the mAb. After cellular internalization, the mAb-ICG conjugate is rapidly degraded. ICG released from the mAb is thus dequenched, thereby becoming an efficient light emitter. Since its fluorescence emission is in the NIR range, the light penetration through tissue is maximal.

A problem with all mAb-ICG conjugates is that, even after intense purification, some proportion of ICG remains noncovalently bound to the mAb. Some of the noncovalent ICG fraction is gradually released from the mAb into the circulation and is excreted through the biliary system as an ICG monomer, leading to high nonspecific background signals, especially in the liver and the intestine. To reduce this effect, we modified the conjugate chemistry of ICG to increase the covalent bonding of ICG to mAb. When a short polyethylene glycol (PEG) linker was inserted, it resulted in bifunctional ICG derivatives (ICG-PEG4-Sulfo-OSu and ICG-PEG8-Sulfo-OSu), which are more efficient to produce a covalent linkage between ICG and the mAb, thus reducing background signals in a mouse xenograft model.[12] However, the addition of PEGs may reduce the binding affinity of the minibody, thus creating a potential trade-off.

Herein, we describe the results of an antiprostate specific membrane antigen (PSMA) minibody-ICG conjugate and demonstrate the effects on imaging efficacy of using short PEG linkers on the ICG.

By adding 1% SDS to dye-conjugated PSMA-MBs, the following dequenching capacities were observed: 36.3-, 16.9-, 6.2-, and 1.4-fold for PSMA-MB-ICG, PSMA-MB-PEG4-ICG, PSMA-MB-PEG8-ICG, and PSMA-MB-IR700, respectively (Figure 1A). As defined by SDS-PAGE, the fraction of covalently bound ICG to PSMA-MB were 16.8%, 67.6%, 67.8%, and 73.4% for PSMA-MB-ICG, PSMA-MB-PEG4-ICG, PSMA-MB-PEG8-ICG, and PSMA-MB-IR700, respectively (Figure 1B). The dissociated ICG was observed in the small molecule fraction. The conjugation ratio of dyes to PSMA-MB was 3.5, 3.0, 2.6, and 4.1 for PSMA-MB-ICG, PSMA-MB-PEG4-ICG, PSMA-MB-PEG8-ICG, and PSMA-MB-IR700, respectively.

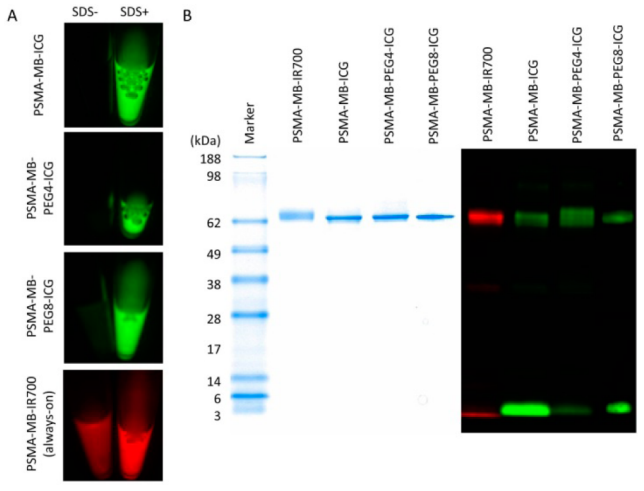

Figure 1. (A) Quenched (left) and chemically dequenched (right) PSMA-MB-ICG, PSMA-MB-PEG4-ICG, PSMA-MB-PEG8-ICG, and PSMA-MB-IR700. (B) Validation of the covalent conjugation of ICG and IR700 to antibody by SDS-PAGE (left, colloidal blue staining; right, fluorescence).

Fluorescence-activated cell sorting flow cytometry showed binding of dye-conjugated PSMA-MBs to the cell line expressing PSMA (Figure 2A–C). PSMA-MB-PEG4-ICG, PSMA-MB-PEG8-ICG, and PSMA-MB-IR700 showed binding affinity to PSMA-positive cells and subsequent dequenching at 1 h after coincubation, and this increased at 6 h. PSMA-MB-ICG showed high binding affinity to PSMA-positive cells and subsequent dequenching at 6 h but little at 1 h, and some affinity also to PSMA-negative cells and subsequent degradation at 6 h after coincubation. Microscopy studies (Figure 2D) using PSMA-MB-ICG showed fluorescence signal in endolysosomes within both of the PSMA-positive and negative cells 6 h after incubation regardless of high dequenching capacity of this probe. On the other hand, PSMA-MB-PEG4-ICG and PSMA-MB-PEG8-ICG showed minimal signal in PSMA-negative cells and significantly higher signal in PSMA-positive cells.

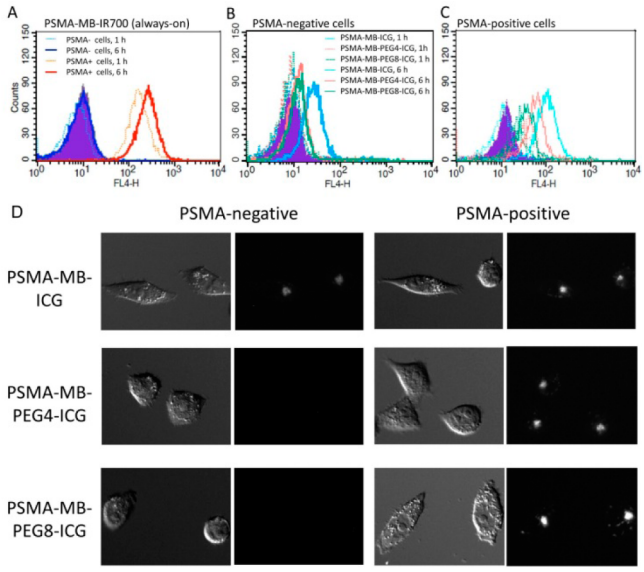

Figure 2. (A) Always-on probe, PSMA-MB-IR700, shows specific binding to PSMA-positive cells at 1 and 6 h after coincubation. Results for PSMA-negative (B) and positive (C) cell lines at 1 or 6 h after incubation with PSMA-MB-ICG, PSMA-MB-PEG4-ICG, and PSMA-MB-PEG8-ICG also show binding affinity to PSMA-positive cells and dequenching. Nonspecific binding is shown with PSMA-MB-ICG, suggesting free ICG formation. (D) PSMA-positive and -negative cells were incubated with PSMA-MB-ICG, PSMA-MB-PEG4-ICG, and PSMA-MB-PEG8-ICG for 6 h.

Figure 3 show the images and quantitative assessment of PSMA-positive and -negative tumor-bearing mice administered PSMA-MB-ICG, PSMA-MB-PEG4-ICG, PSMA-MB-PEG8-ICG, and PSMA-MB-IR700 using the 700 and 800 nm fluorescence channel of the fluorescence camera for IR700 and ICG, respectively. PSMA-positive tumors were visualized by 6 h and at all later time points. PSMA-negative tumors were also observed by 6 h, but their fluorescence signal declined earlier than that of PSMA-positive tumors and signal was reduced to background levels. PSMA-MB-ICG showed higher background signals, especially in the liver and intestine (Figure 3A,B) and the hepatic signal was significantly higher than that seen with PSMA-MB-PEG4-ICG or PSMA-MB-PEG8-ICG (Figure 3C). Therefore, the fluorescence signal ratio of PSMA-

dx.doi.org/10.1021/ml400533y | ACS Med. Chem. Lett. 2014, 5, 411–415

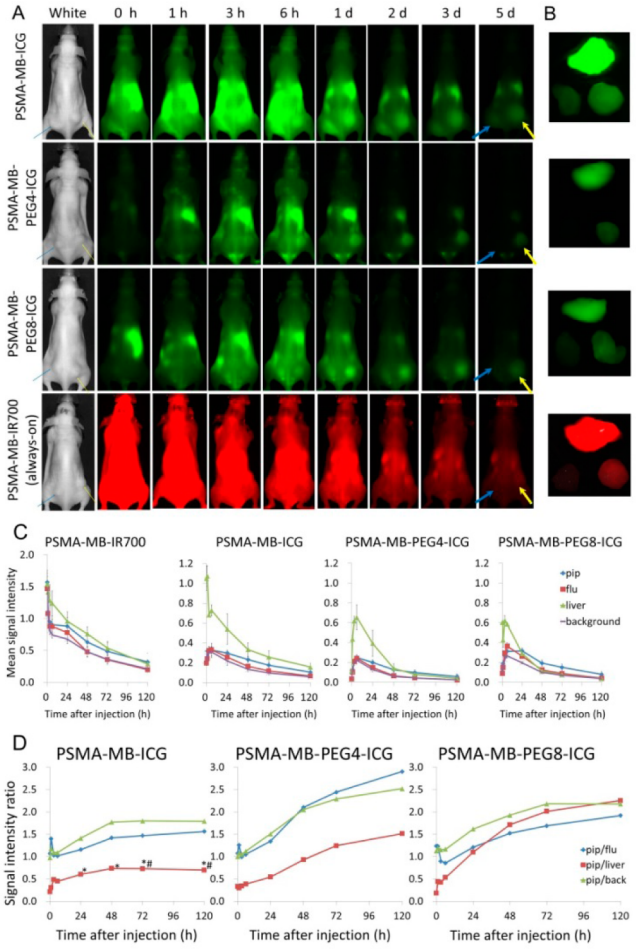

Figure 3. (A) In vivo serial fluorescence images of PSMA-positive (yellow arrows) and -negative (blue arrows) tumors in mice injected with PSMA-MB-ICG, PSMA-MB-PEG4-ICG, PSMA-MB-PEG8-ICG, and PSMA-MB-IR700. (B) Ex vivo fluorescence images of the liver (upper), PSMA-positive (bottom right), and PSMA-negative (bottom left) tumors obtained 5 d after injection of PSMA-MBs. (C) Mean signal intensity of PSMA-positive (pip), negative tumors (flu), liver, and the body (background) of mice after injection of PSMA-MB-IR700 (always-on probe), PSMA-MB-ICG, PSMA-MB-PEG4-ICG, and PSMA-MB-PEG8-ICG. (D) The signal intensity ratio of PSMA-positive tumor to negative tumor (pip/flu), liver (pip/liver), or background (pip/back) after injection of PSMA-MB-ICG, PSMA-MB-PEG4-ICG, and PSMA-MB-PEG8-ICG is shown. Data are means ± s.e.m. (n = 3). #P < 0.05 vs PSMA-PEG4-ICG group. *P < 0.05 vs PSMA-MB-PEG8-ICG group.

positive tumors to other organs after injection of PSMA-MB-ICG tended to be lower than that of PSMA-MB-PEG4-ICG or PSMA-MB-PEG8-ICG, and statistical significance was shown in the ratio to the liver signal (Figure 3D). Although PSMA-MB-IR700 (always-on probe) showed high background signal especially in the abdominal region suggesting blood pool and uptake in the liver and kidneys at early time points, signal intensity in the PSMA-positive tumors remained sturdy and declined in the other organs, and thus, the fluorescence ratio of PSMA-positive tumors to background increased gradually.

^{125}I-PSMA-MB-PEG8-ICG showed a similar biodistribution to ^{125}I-PSMA-MB. Both labeled PSMA-MBs mainly distributed to the kidney, lung, heart, liver, and spleen at 1 h after injection and the radioactivity in those organs gradually decreased thereafter (Figure 4). The radioactivity in other organs tended

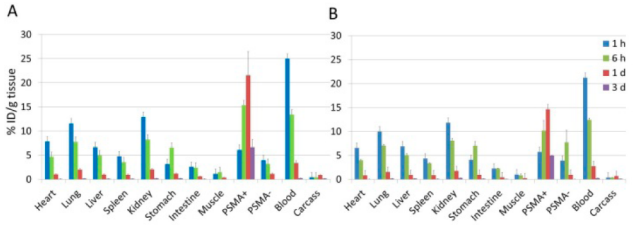

Figure 4. In vivo biodistribution of radioactivity at 1 h, 6 h, 1 d, and 3 d after injection of ^{125}I-PSMA-MB (A) and ^{125}I-PSMA-MB-PEG8-ICG (B) in mice with PSMA-positive and negative tumors. Radioactivity is expressed as % injected dose/g (%ID/g) of tissue. Data are represented as mean ± s.e.m. (n = 5).

to decline over time as well, while uptake in the stomach showed transient increases at 6 h. High TBRs were seen with PSMA-MBs in PSMA-positive tumors up to 3 d, while the radioactivity in PSMA-negative tumors declined much more rapidly.

An anti-PSMA mAb-ICG conjugate demonstrated highly specific detection of PSMA-positive tumors from 1 to 10 d after intravenous injection in a mouse xenograft model.[13] However, at least one day was required for sufficient background to be cleared to allow for imaging. This delay is undesirable from a clinical translational viewpoint since it might require a separate patient visit. In order to speed up the pharmacokinetics to enable same-day imaging, we used an anti-PSMA minibody instead of the full antibody and then synthesized three-ICG derivative conjugates as activatable optical probes. All depicted PSMA-positive tumors with significantly higher contrast than "always-on" probes beginning 6 h post injection (p.i.) and extending up to 5 d p.i.

Antibody fragments are known to have more rapid clearance and better penetration into the tumor.[14,15] Previously, we performed in vivo fluorescence imaging using an anti-PSMA diabody conjugated with ICG derivatives, but this resulted in unexpectedly high background signals.[16] Biodistribution studies of ^{125}I-labeled diabodies showed significantly higher activity in the kidney at 1 h and relatively high activity in the stomach at 6 h after injection, suggesting that the diabodies were taken up rapidly in the renal tubular epithelial cells and catabolized (dehalogenated). Then, a large amount of released ICG was thought to bind to plasma protein, remain in the blood, and gradually be excreted via the hepatobiliary system. However, ^{125}I-labeled PSMA-MBs did not show significant accumulation in the kidney nor significant increase of activity in the stomach at 6 h. This suggests that minibody-based ICG conjugates are not significantly taken up and catabolized in the kidney, unlike diabodies, thereby resulting in their pharmacokinetics favorable for achieving high TBRs.

The MB-PEG-ICG conjugates have several advantages over other optical probes. ICG has been used clinically for many years and its safety has been confirmed.[17,18] In addition, ICG derivatives are remarkably efficient as activatable probes: bifunctional ICG derivatives are highly quenchable, and the probes can be turned "on" only at the target tissue by employing signal activation mechanisms such as dequenching.[19] Finally, the biocompatibility of PEG is well-known and has been widely used in clinical products.[20] Although it has not been clinically approved, the minibody has shown promise as an imaging agent. A ^{123}I-labeled minibody was administered to patients with advanced colorectal cancer and demonstrated tumor targeting and a faster clearance in comparison with

dx.doi.org/10.1021/ml400533y | ACS Med. Chem. Lett. 2014, 5, 411−415

labeled intact antibodies without drug-related adverse reactions.[21] Although formal safety studies of the final conjugates will be required, it is encouraging that each component of the conjugate has a favorable toxicity profile.

Site-specific conjugation is generally advantageous for labeling antibodies or antibody-fragments in order to obtain monodispersed products with high yield and minimal loss of immunoreactivity. However, efficiently quenched and activatable ICG conjugates with antibodies or antibody-fragments are synthesized better with the random conjugation to lysine using the *N*-hydroxysuccinimidyl (NHS) ester than with the site-specific conjugation via sulfohydryl group. Therefore, even when designing GMP-grade MB-ICG conjugates for clinical trials, the NHS conjugation chemistry with a PEG4 linker is employed.

A potential alternative for activatable in vivo imaging is the use of fluorescent proteins, which are excellent endogenous fluorescence emitters for depicting various biological processes both in vitro and in vivo.[22] Some of these studies were performed with orthotopic tumor models, which were better models than subcutaneous xenografts.[23] These technologies might have unique clinical benefits for detecting cancer based on biological features. However, for common medical application, the requirement that fluorescence proteins are transduced by virus-mediated in vivo gene transfection, makes this approach less practical.

In conclusion, we conjugated bifunctional ICG derivatives with and without short PEG linkers to an anti-PSMA minibody and these conjugates successfully visualized PSMA positive tumors at earlier time points than mAb-based conjugates. The addition of short PEG linkers significantly increased the percentage of covalent bonding of ICG to minibody; this improved tumor-to-background ratios by decreasing release of ICG monomers that are especially excreted through the liver. Thus, minibody-based activatable optical probes could be a good alternative to full antibody-based optical probes.

EXPERIMENTAL PROCEDURES

Synthesis of Fluorophore Conjugated PSMA-MBs. PSMA-MB (0.5 mg, 6.25 nmol) was incubated with ICG-Sulfo-OSu (69.8 μg, 75.0 nmol), ICG-PEG4-Sulfo-OSu (44.2 μg, 37.5 nmol), ICG-PEG8-Sulfo-OSu (101.5 μg, 75.0 nmol), or IR700 (73.3 μg, 37.5 nmol) in 0.1 M Na_2HPO_4 (pH 8.6) at room temperature for 30 min, followed by purification with a size exclusion Sephadex G-25 M column (PD-10; GE Healthcare, Piscataway, NJ).

Determination of Quenching Capacity in Vitro. The quenching capacity of each conjugate was investigated by denaturation by SDS as described previously.[12] Briefly, the conjugates were incubated with 1% SDS in PBS for 15 min at room temperature. The change in fluorescence intensity for each conjugate was measured with an in vivo imaging system (Maestro, CRi Inc., Woburn, MA).

Flow Cytometry. Fluorescence signal from PC3-PSMA-positive and -negative cells after incubation with ICG- or IR700-conjugated PSMA-MBs was measured using a FACSCalibur flow cytometer (BD Biosciences, San Jose, CA) and CellQuest software (BD Biosciences).

Fluorescence Microscopy Studies. PSMA-positive or negative cells (1×10^4) were plated on a covered glass-bottomed culture well and incubated for 16 h. Then, PSMA-MB-ICG, PSMA-MB-PEG4-ICG, or PSMA-MB-PEG8-ICG was added to the medium (5 μg/mL), and the cells were incubated for 6 h. Cells were washed once with PBS, and fluorescence microscopy was performed using an Olympus BX61 microscope (Olympus America, Inc., Melville, NY).

Animal Tumor Model. All procedures were carried out in compliance with the Guide for the Care and Use of Laboratory Animal Resources (1996), National Research Council, and approved by the local Animal Care and Use Committee. Six to eight week old female homozygote athymic nude mice were purchased from Charles River (NCI-Frederick, MD). Both receptor positive and negative tumor cell lines were implanted in the same mouse: 2×10^6 PSMA-positive cells and negative cells suspended in PBS were injected subcutaneously in the right and left dorsum of the mice, respectively.

In Vivo Imaging Studies Targeting for PSMA. Each probe (PSMA-MB-ICG, PSMA-MB-PEG4-ICG, PSMA-MB-PEG8-ICG, and PSMA-MB-IR700) was diluted in 200 μL PBS at the dose of 25 μg and injected into mice bearing both PSMA-positive and -negative tumors. The fluorescence images were obtained with a Pearl Imager (LI-COR Biosciences, Lincoln, NE) using the 700 and 800 nm fluorescence channel for IR700 and ICG, respectively, at 0, 1, 3, and 6 h and, 1, 2, 3, and 5 d after injection.

Biodistribution Study. PSMA-positive and -negative tumor-bearing mice were divided into two groups ($n = 5$) with approximately equal distributions of tumor sizes on the day of study, 5 d after inoculation of the cells. ^{125}I-PSMA-MB or ^{125}I-PSMA-MB-PEG8-ICG (37 kBq/1.0 μg/200 μL in PBS/mouse) was injected, and the biodistribution was determined at 1 and 6 h, and 1 and 3 d after injection. Data were calculated as the percentage injected dose per gram of tissue (%ID/g).

Statistical Analysis. Quantitative data were expressed as mean ± s.e.m. Means were compared using two-way repeated measures ANOVA with the Bonferroni correction of multiple comparisons. *P*-value of <0.05 was considered statistically significant.

ASSOCIATED CONTENT

Supporting Information

Detailed experimental procedures. This material is available free of charge via the Internet at http://pubs.acs.org.

AUTHOR INFORMATION

Corresponding Author

*(H.K.) Phone: 301-435-4086. Fax: 301-402-3191. E-mail: kobayash@mail.nih.gov.

Author Contributions

R.W. conducted experiments, performed analysis, and wrote the manuscript; K.S., H.H., T.H., T.N., I.K., and C.H.P. conducted experiments and performed analysis; A.M.W. and P.L.C. wrote the manuscript and supervised the project; and H.K. planned and initiated the project, designed and conducted experiments, wrote the manuscript, and supervised the entire project.

Funding

This research was supported by the Intramural Research Program of the NCI/NIH. This project has been funded in whole or in part with federal funds from the National Cancer Institute, National Institutes of Health, under Contract No. HHSN261200800001E.

Notes

The authors declare no competing financial interest.

ACKNOWLEDGMENTS

We thank Drs. Derek Bartlett, Christian P. Behrenbruch, and Jean Gudas in the ImaginAb Inc. for their technical and administrative assistances.

ABBREVIATIONS

PSMA, prostate-specific membrane antigen; MB, minibody; TBR, target-to-background ratios; ICG, indocyanine green; PEG, polyethylene glycol; mAb, monoclonal antibody; NIR, near-infrared; ROI, region of interest; %ID/g, percentage injected dose per gram of tissue

REFERENCES

(1) Frangioni, J. V. New technologies for human cancer imaging. *J. Clin. Oncol.* **2008**, *26*, 4012−4021.

(2) Wallace, M. B.; Sullivan, D.; Rustgi, A. K. Advanced imaging and technology in gastrointestinal neoplasia: Summary of the AGA-NCI Symposium October 4−5, 2004. *Gastroenterology* **2006**, *130*, 1333−1342.

(3) Van Dam, G. M.; Themelis, G.; Crane, L. M.; Harlaar, N. J.; Pleijhuis, R. G.; Kelder, W.; Sarantopoulos, A.; de Jong, J. S.; Arts, H. J.; van der Zee, A. G.; Bart, J.; Low, P. S.; Ntziachristos, V. Intraoperative tumor-specific fluorescence imaging in ovarian cancer by folate receptor-α targeting: first in-human results. *Nat. Med.* **2011**, *17*, 1315−1319.

(4) Reichert, J. M. Marketed therapeutic antibodies compendium. *MAbs* **2012**, *4*, 413−415.

(5) Wu, A. M.; Senter, P. D. Arming antibodies: prospects and challenges for immunoconjugates. *Nat. Biotechnol.* **2005**, *23*, 1137−1146.

(6) Wu, A. M. Engineered antibodies for rapid clinical imaging of cell surface markers. *Am. Assoc. Cancer Res. Educ. Book* **2012**, 221−225.

(7) Sundaresan, G.; Yazaki, P. J.; Shively, J. E.; Finn, R. D.; Larson, S. M.; Raubitschek, A. A.; Williams, L. E.; Chatziioannou, A. F.; Gambhir, S. S.; Wu, A. M. ^{124}I-labeled engineered anti-CEA minibodies and diabodies allow high-contrast, antigen-specific small-animal PET imaging of xenografts in athymic mice. *J. Nucl. Med.* **2003**, *44*, 1962−1969.

(8) Okafsen, T.; Sirk, S. J.; Olma, S.; Shen, C. K.; Wu, A. M. ImmunoPET using engineered antibody fragments: fluorine-18 labeled diabody for same-day imaging. *Tumor Biol.* **2012**, *33*, 669−677.

(9) Kobayashi, H.; Longmire, M. R.; Ogawa, M.; Choyke, P. L. Rational chemical design of the next generation of molecular imaging probes based on physics and biology; mixing modalities, colors and signals. *Chem. Soc. Rev.* **2011**, *40*, 4626−4748.

(10) Kobayashi, H.; Ogawa, M.; Alford, R.; Choyke, P. L.; Urano, Y. New strategies for fluorescent probe design in medical diagnostic imaging. *Chem. Rev.* **2010**, *110*, 2620−2640.

(11) Ogawa, M.; Kosaka, N.; Choyke, P. L.; Kobayashi, H. In vivo molecular imaging of cancer with a quenching near infrared fluorescent probe using conjugates of monoclonal antibodies and indocyanine green. *Cancer Res.* **2009**, *69*, 1268−1272.

(12) Sano, K.; Nakajima, T.; Miyazaki, K.; Ohuchi, Y.; Ikegami, T.; Choyke, P. L.; Kobayashi, H. Short PEG-linkers improve the performance of targeted, activatable monoclonal antibody-indocyanine green optical imaging probes. *Bioconjugate Chem.* **2013**, *24*, 811−816.

(13) Nakajima, T.; Mitsunaga, M.; Bander, N. H.; Heston, W. D.; Choyke, P. L.; Kobayashi, H. Targeted, activatable, in vivo fluorescence imaging of prostate-specific membrane antigen (PSMA) positive tumors using the quenched humanized J591 antibody-indocyanine green (ICG) conjugate. *Bioconjugate Chem.* **2011**, *22*, 1700−1705.

(14) Buchegger, F.; Haskell, C. M.; Schreyer, M.; Scazziga, B. R.; Randin, S.; Carrel, S.; Mach, J. P. Radiolabeled fragments of monoclonal antibodies against carcinoembryonic antigen for localization of human colon carcinoma grafted into nude mice. *J. Exp. Med.* **1983**, *158*, 413−427.

(15) Yokota, T.; Milenic, D. F.; Whitlow, M.; Schlom, J. Rapid tumor penetration of a single-chain Fv and comparison with other immunoglobulin forms. *Cancer Res.* **1992**, *52*, 3402−3408.

(16) Sano, K.; Nakajima, T.; Ali, T.; Bartlett, D. W.; Wu, A. M.; Kim, I.; Paik, C. H.; Choyke, P. L.; Kobayashi, H. Activatable fluorescent cys-diabody conjugated with indocyanine green derivative: consideration of fluorescent catabolite kinetics on molecular imaging. *J. Biomed. Opt.* **2013**, *18*, 101304.

(17) Stanga, P.; Lim, J. I.; Hamilton, P. Indocyanine green angiography in chorioretinal diseases: indications and interpretation: an evidence-based update. *Opthalmology* **2003**, *110*, 22−24.

(18) Seyama, Y.; Kokudo, N. Assessment of liver function for safe hepatic resection. *Hepatol. Res.* **2009**, *39*, 107−116.

(19) Weissleder, R.; Tung, C. H.; Mahmood, U.; Bogdanov, A., Jr. In vivo imaging of tumors with protease-activated near-infrared fluorescent probes. *Nat. Biotechnol.* **1999**, *17*, 375−378.

(20) Banerjee, S. S.; Aher, N.; Patil, R.; Khandare, J. Poly(ethylene glycol)-prodrug conjugates: concept, design, and applications. *J. Drug Delivery* **2012**, 103973.

(21) Wong, J. Y. C.; Chu, D. V.; Williams, L. E.; Yamauchi, D. M.; Ikle, D. N.; Kwok, C. S.; Liu, A.; Wilczynski, S.; Colcher, D.; Yazaki, P. J.; Shively, J. E.; Wu, A. M.; Raubitschek, A. A. Pilot trial evaluating an ^{123}I-labeled 80-kilodalton engineered anticarcinoembryonic antigen antibody fragment (cT84.66 minibody) in patients with colorectal cancer. *Clin. Cancer Res.* **2004**, *10*, 5014−5021.

(22) Bouvet, M.; Hoffman, R. M. Glowing tumors make for better detection and resection. *Sci. Transl. Med.* **2011**, *3*, 110fs110.

(23) Yang, M.; Jiang, P.; Yamamoto, N.; Li, L.; Geller, J.; Moossa, A. R.; Hoffman, R. M. Real-time whole-body imaging of an orthotopic metastatic prostate cancer model expressing red fluorescent protein. *Prostate* **2005**, *62*, 374−379.